

Stability in a scalar differential equation with multiple, distributed time delays

Sue Ann Campbell*

*Department of Applied Mathematics and Centre for Theoretical Neuroscience,
University of Waterloo, Waterloo, Ontario, N2L 3G1, Canada*

Israel Ncube

*College of Engineering, Technology & Physical Sciences, Department of Mathematics,
Alabama A & M University, 4900 Meridian Street N., Huntsville, AL 35762, U.S.A.*

arXiv:1611.00207v2 [math.DS] 2 Feb 2017

Abstract

We consider a linear scalar delay differential equation (DDE), consisting of two arbitrary distributed time delays. We formulate necessary conditions for stability of the trivial solution which are independent of the distributions. For the case of one discrete and one gamma distributed delay, we give an explicit description of the region of stability of the trivial solution and discuss how this depends on the model parameters.

Keywords: delay differential equations, distributed delay, stability boundaries
2000 MSC: 34K20

1. Introduction

Distributed time delays arise in models for a variety of applications including population dynamics [1, 2, 3, 4], blood cell dynamics [5, 6], neuronal models [7, 8], and coupled oscillators [9, 10]. Although many of these models include only a single time delay, this often results from some simplification in the model set up. As an example, it is common to assume that all of the time delays are identical [7] or to neglect relatively smaller time delays [3]. The stability of equilibria in models with two discrete time delays has been studied extensively [11, 12, 13, 14]. It has been shown that the presence of two time delays can lead to phenomena such as stability switching and the existence of codimension two bifurcation points [11, 14]. In this article, we investigate such phenomena in a model with two distributed time delays. We focus our attention on the following scalar delay differential equation (DDE) with a linear decay:

$$\dot{x}(t) = -kx(t) + \alpha \int_0^\infty x(t - \tau) f_\alpha(\tau) d\tau + \beta \int_0^\infty x(t - \tau) f_\beta(\tau) d\tau, \quad (1)$$

where k , α , β are real numbers, $f_\alpha(T)$ and $f_\beta(T)$ are *arbitrary* distributions, satisfying

$$\int_0^\infty f_\alpha(s) ds = 1 = \int_0^\infty f_\beta(s) ds.$$

*Corresponding author

Email addresses: sacampbell@uwaterloo.ca (Sue Ann Campbell), Ncube.Israel@gmail.com (Israel Ncube)

We note that (1) is a delay differential equation with infinite delay. Thus the appropriate phase space is $C_{0,\rho}((-\infty, 0], \mathbf{R})$ where ρ is a positive constant [15, 16, 17]. This is the Banach space of functions $\psi : (-\infty, 0] \rightarrow \mathbf{R}$ such that $e^{\rho\theta}\psi(\theta)$ is continuous and

$$\lim_{\theta \rightarrow -\infty} e^{\rho\theta}\psi(\theta) = 0,$$

with norm $\|\psi\|_{\infty,\rho} = \sup_{\theta \leq 0} e^{\rho\theta}\psi(\theta)$. In this space, we need the following additional conditions on the distributions

$$\int_0^{\infty} e^{\rho s} f_{\alpha}(s) ds < \infty, \quad \int_0^{\infty} e^{\rho s} f_{\beta}(s) ds < \infty.$$

Since equation (1) is linear it will have a unique solution for any initial function $\phi \in C_{0,\rho}((-\infty, 0], \mathbf{R})$ [15, 16, 17].

Stability with general distributions has been studied by some authors, but generally only with a single delay [18, 5, 19, 20, 21]. In particular we note the work of Anderson [22, 23] which studies stability properties of linear, scalar differential equation with a single distributed time delay, in terms of the moments of the distribution.

Stability in the presence of multiple distributed delays has been studied in some models, generally by fixing the distributions to some specific form [24, 25, 26, 27, 28]. An exception is the work of Faria and Oliveira [2] which studies the global stability of equilibria in a class of Lotka-Volterra models with multiple distributed delays having finite maximum delay. They give conditions on the interaction coefficients of the system which guarantee asymptotic stability for any distribution.

Various specific time delay kernels have been used in the literature. The two most commonly used ones are the *weak* and the *strong* kernels (gamma distributions), given by $f(s) = re^{-rs}$ and $f(s) = r^2 se^{-rs}$, with $r > 0$, respectively. It is well-known (see [29] and [30], for instance) that the average time delays associated with the weak and the strong delay kernels are given by $T = \frac{1}{r}$ and $T = \frac{2}{r}$, respectively. Equation (1) would occur in the linearisation about an equilibrium point for the models of [11, 12] and [14, 26] if the discrete delays were replaced by distributed delays.

Making the change of variables $\tilde{x} = x$, $\tilde{t} = kt$, and defining new parameters by $\tilde{\alpha} = \frac{\alpha}{k}$, $\tilde{\beta} = \frac{\beta}{k}$, $T = k\tau$, and new distributions

$$g_{\alpha}(T) = \frac{1}{k} f_{\alpha}\left(\frac{T}{k}\right), \quad g_{\beta}(T) = \frac{1}{k} f_{\beta}\left(\frac{T}{k}\right),$$

we rescale (1) to get

$$\dot{x}(t) = -x(t) + \alpha \int_0^{\infty} x(t-T)g_{\alpha}(T) dT + \beta \int_0^{\infty} x(t-T)g_{\beta}(T) dT, \quad (2)$$

where, for notational tractability, we have dropped the tilde's.

In this paper, we will investigate the stability of the trivial solution of (2) by adopting direct analysis of the associated characteristic equation. The paper is organised as follows. In Section 2, we formulate some necessary distribution-independent conditions for stability of the trivial solution. In Section 3, we describe some distribution-specific mechanisms by which bifurcation curves evolve in an appropriate parameter space, and how this has an effect on the region of stability. Section 3.3 discusses how stability changes as bifurcation curves are traversed in the parameter space characterised by β and the mean delay of g_{β} .

2. Distribution-independent stability

In equation (2), we make the ansatz that $x(t) \simeq ce^{\lambda t}$, $c \in \mathbb{R}$, $\lambda \in \mathbb{C}$, to obtain the associated characteristic equation, which is given by

$$D(\lambda) := \lambda + 1 - \alpha \int_0^\infty e^{-\lambda T} g_\alpha(T) dT - \beta \int_0^\infty e^{-\lambda T} g_\beta(T) dT = 0. \quad (3)$$

It is well-known [15] that the trivial solution of (2) will be asymptotically stable if all the roots of the characteristic equation have negative real parts and unstable if at least one root has a positive real part. In this section we focus on deriving conditions for stability and instability which do not depend on the particular distributions that occur in the equation.

Theorem 2.1. *If $\alpha + \beta > 1$, then the trivial solution of (2) is unstable.*

Proof. Assume that λ is a real root of (3). Then we have

$$\begin{aligned} D(\lambda) &= \lambda + 1 - \alpha \int_0^\infty e^{-\lambda T} g_\alpha(T) dT - \beta \int_0^\infty e^{-\lambda T} g_\beta(T) dT \\ &\geq \lambda + 1 - |\alpha| \int_0^\infty g_\alpha(T) dT - |\beta| \int_0^\infty g_\beta(T) dT \\ &\geq \lambda + 1 - |\alpha| - |\beta|. \end{aligned}$$

Consequently, for λ real and sufficiently large, we conclude that $D(\lambda) > 0$. Furthermore, we note that

$$D(0) = 1 - \alpha \int_0^\infty g_\alpha(T) dT - \beta \int_0^\infty g_\beta(T) dT = 1 - (\alpha + \beta) < 0.$$

Thus, since $D(\lambda)$ is continuous, we conclude that it has a root with positive real part. ■

Let τ_α and τ_β be the mean delays of g_α and g_β , respectively. That is,

$$\tau_\alpha = \int_0^\infty T g_\alpha(T) dT, \quad \tau_\beta = \int_0^\infty T g_\beta(T) dT.$$

Theorem 2.2. *Assume that $D(\lambda)$ is analytic in $\text{Re}(\lambda) > -d$ for some $d > 0$. The trivial solution of (2) is asymptotically stable if $|\alpha| + |\beta| < 1$.*

Proof. We will prove this result by the use of Rouché's Theorem [31, p. 313]. To begin, let

$$f_1(\lambda) = \lambda + 1 - \alpha \int_0^\infty e^{-\lambda T} g_\alpha(T) dT \quad f_2(\lambda) = -\beta \int_0^\infty e^{-\lambda T} g_\beta(T) dT,$$

and consider the contour in the complex plane, $C = C_1 \cup C_2$, given by

$$C_1 : \lambda = Re^{i\theta}, \quad -\frac{\pi}{2} \leq \theta \leq \frac{\pi}{2} \quad C_2 : \lambda = iy, \quad -R \leq y \leq R,$$

where $R \in \mathbb{R}$. On C_1 , we have that

$$\begin{aligned}
|f_2(\lambda)| &= \left| -\beta \int_0^\infty e^{-RTe^{i\theta}} g_\alpha(T) dT \right| \\
&\leq |\beta| \int_0^\infty e^{-RT \cos(\theta)} |e^{-iRT \sin(\theta)}| g_\alpha(T) dT \\
&\leq |\beta| \int_0^\infty g_\alpha(T) dT \\
&= |\beta|.
\end{aligned}$$

Furthermore, we note that $f_1(\lambda) = Re^{i\theta} + 1 - \alpha G_\alpha$, where

$$\begin{aligned}
G_\alpha &= \int_0^\infty [\cos(RT \sin(\theta)) + i \sin(RT \sin(\theta))] e^{-RT \cos(\theta)} g_\alpha(T) dT \\
&= G_\alpha^R + iG_\alpha^I.
\end{aligned}$$

Hence, we obtain

$$\begin{aligned}
|f_1(\lambda)| &= \sqrt{(R \cos(\theta) + 1 + G_\alpha^R)^2 + (R \sin(\theta) + G_\alpha^I)^2} \\
&= \sqrt{R^2 + 2R \cos(\theta) + 1 + |G_\alpha|^2 + 2G_\alpha^R + 2R[\cos(\theta)G_\alpha^R + \sin(\theta)G_\alpha^I]} \\
&= \sqrt{R^2 + 2R \cos(\theta) + 1 + |G_\alpha|^2 + 2G_\alpha^R + 2R \int_0^\infty \cos(\theta + RT \sin(\theta)) e^{-RT \cos(\theta)} g_\alpha(T) dT} \\
&\geq \sqrt{R^2 + 1 - 2 - 2R} \\
&= \sqrt{(R - 1)^2 - 2}.
\end{aligned}$$

Thus, for R sufficiently large, $|f_1(\lambda)| > |f_2(\lambda)|$ on C_1 . On C_2 , we have that

$$\begin{aligned}
|f_2(\lambda)| &= \left| -\beta \int_0^\infty e^{-iyT} g_\alpha(T) dT \right| \\
&\leq |\beta| \int_0^\infty g_\alpha(T) dT \\
&= |\beta|.
\end{aligned}$$

Additionally, it is crucial to note that if $|\alpha| < 1$, then

$$\begin{aligned}
|f_1(\lambda)| &= \left| iy + 1 - \alpha \int_0^\infty e^{-iyT} g_\alpha(T) dT \right| \\
&= \sqrt{(1 - \alpha \int_0^\infty \cos(yT) g_\alpha(T) dT)^2 + (y + \alpha \int_0^\infty \sin(yT) g_\alpha(T) dT)^2} \\
&\geq \sqrt{(1 - |\alpha|)^2} \\
&= 1 - |\alpha|.
\end{aligned}$$

As a result, if $1 - |\alpha| > |\beta|$, then $|f_1(\lambda)| > |f_2(\lambda)|$ on C_2 . We note that if $\alpha \neq 0$, and $\beta \neq 0$, then both f_1 and f_2 do not reduce to zero anywhere on C . Thus, by Rouché's Theorem, if $1 - |\alpha| > |\beta| > 0$ and R is sufficiently large, then $f_1(\lambda)$ and $D(\lambda) = f_1(\lambda) + f_2(\lambda)$ have the same number of zeroes inside C . In the

limit as $R \rightarrow \infty$, it is easy to see that $f_1(\lambda)$ and $D(\lambda)$ have the same number of zeroes with $\text{Re}(\lambda) > 0$. It has been shown [32] that all the zeroes of $f_1(\lambda)$ have negative real part if $|\alpha| < 1$. This completes the proof. ■

For our final result, we specialise to the situation in which one of the time delays is discrete. That is,

$$g_\alpha(T) = \delta(T - \tau_\alpha). \quad (4)$$

We begin with the following.

Lemma 1. *The function $\omega + \xi \sin(\omega\tau_\alpha) > 0$ for all $\omega > 0$ if, and only if,*

1. $-\frac{1}{\tau_\alpha} \leq \xi \leq 0$,
2. $0 \leq \xi \leq \frac{u^*}{\tau_\alpha}$, where $u^* \approx 4.603$ is the unique positive zero of

$$2\pi - \cos^{-1}\left(-\frac{1}{u}\right) + u \sin\left(2\pi - \cos^{-1}\left[-\frac{1}{u}\right]\right). \quad (5)$$

Proof. Let $S(\omega) = \omega + \xi \sin(\omega\tau_\alpha)$. Clearly, $S(0) = 0$ and $\lim_{\omega \rightarrow \infty} S(\omega) > 0$. Now, $\frac{dS}{d\omega} = 1 + \xi\tau_\alpha \cos(\omega\tau_\alpha)$, which is clearly positive for all $\omega > 0$ if $|\xi\tau_\alpha| < 1$. It follows that $S(\omega) > 0$ for all $\omega > 0$ if $|\xi\tau_\alpha| < 1$.

If $\xi\tau_\alpha = -1$ then $S'(0) = S''(0) = 0$, $S'''(0) > 0$ and $S'(\omega) \geq 0$ for $\omega > 0$. Thus, $S(\omega) > 0$ for all $\omega > 0$ in this case as well. Finally, we note that if $\xi\tau_\alpha < -1$, then $\frac{dS}{d\omega}\big|_{\omega=0} < 0$. The first result follows.

If $\xi > 0$, however, $\frac{dS}{d\omega}\big|_{\omega=0} > 0$ for any value of τ_α . $S(\omega)$ can change sign only if it is zero for some ω . $S(\omega)$ will first become zero when there exists ξ , τ_α , and $\omega^* > 0$ such that $S(\omega^*) = 0$ and $S'(\omega^*) = 0$. In other words, when

$$\begin{aligned} \omega^* + \xi \sin(\omega^* \tau_\alpha) &= 0, \\ 1 + \xi \tau_\alpha \cos(\omega^* \tau_\alpha) &= 0. \end{aligned}$$

A simple rearrangement shows that these equations are equivalent to (5), where $u = \xi\tau_\alpha$. It is straightforward to show that (5) has a unique positive zero, u^* , and that if $\xi > u^*/\tau_\alpha$, then there exists an $\omega > 0$ such that $S(\omega) < 0$. ■

We are now in a position to state our final result.

Theorem 2.3. *Let g_α be given by (4) and assume that $D(\lambda)$ in (3) is analytic in $\text{Re}(\lambda) > -d$ for some $d > 0$. Then the trivial solution of (2) is asymptotically stable if $\alpha < -1$, $\tau_\alpha \leq -1/(2\alpha)$, and $|\beta| < -\alpha - 1$.*

Proof. The proof setup is identical to that of Theorem 2.2, except that $f_1 = \lambda + 1 - \alpha e^{-\lambda\tau_\alpha}$ in the present case. The proof is the same except that on C_2 we have

$$\begin{aligned} |f_1(\lambda)| &= \sqrt{1 + \alpha^2 - 2\alpha \cos(y\tau_\alpha) + y(y + 2\alpha \sin(y\tau_\alpha))} \\ &\geq \sqrt{(1 - |\alpha|)^2} \\ &= -\alpha - 1, \end{aligned}$$

where we have used Lemma 1 to show that the term $y(y + 2\alpha \sin(y\tau_\alpha))$ is non-negative if $\tau_\alpha \leq -1/(2\alpha)$. We note that all of the roots of $f_1(\lambda)$ have negative real parts if

$$\alpha < -1 \quad \text{and} \quad \tau_\alpha \leq -\frac{1}{2\alpha}$$

[32]. The rest of the proof proceeds in a manner analogous to the proof of Theorem 2.2. ■

The results of this section are illustrated in Figure 1. The unshaded regions of Figure 1 are regions in which we do not know whether the trivial solution is stable or not. To investigate this further, we need more information about the distributions. This is the focus of Section 3.

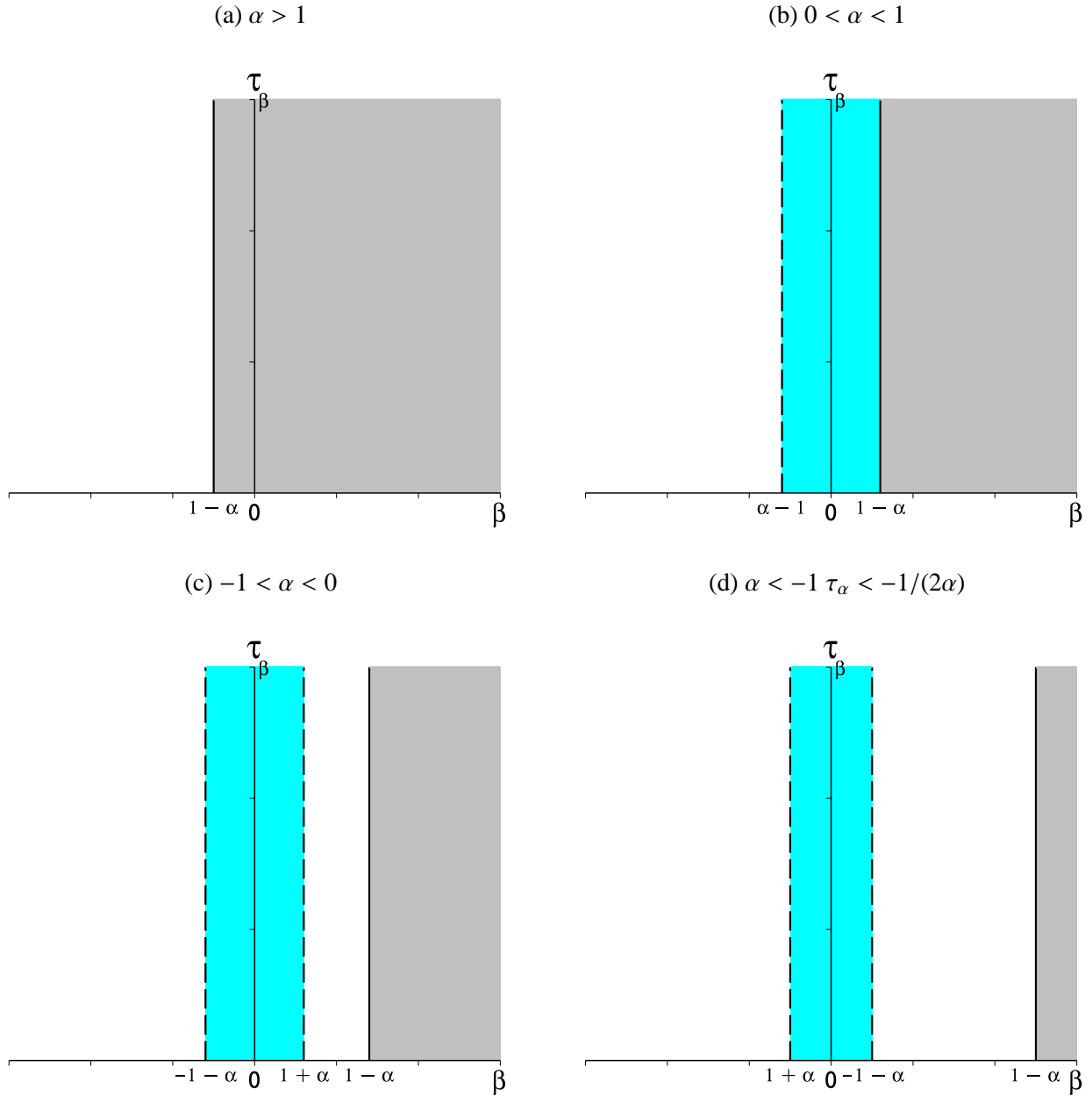


Figure 1: Illustration of results in the (β, τ_β) plane. Regions shaded in grey correspond to the region of instability described in Theorem 2.1. Regions shaded in cyan correspond to the regions of stability described in Theorem 2.2 (b),(c), and Theorem 2.3 (d).

3. Stability Boundaries

The last section described regions in parameter space where the trivial solution is unstable and regions where it is asymptotically stable regardless of the choice of distribution. However, these regions do not cover the entire parameter space; indeed, there are regions where the stability is unknown. This issue will be addressed in the rest of the paper. We will attempt to give a concrete description of the complete stability region in the (β, τ_β) parameter space, for the following choices of distributions:

$$g_\alpha(T) = \delta(T - \tau_\alpha),$$

$$g_\beta(T) = \frac{a^m T^{m-1} e^{-aT}}{(m-1)!}, \quad a > 0, \quad m > 0, \quad (6)$$

so the first time delay is discrete and the second is a gamma distribution. With these choices, equation (2) becomes

$$\dot{x}(t) = -x(t) + \alpha x(t - \tau_\alpha) + \frac{\beta a^m}{(m-1)!} \int_0^\infty x(t-T) T^{m-1} e^{-aT} dT, \quad (7)$$

and the mean delay of g_β is

$$\tau_\beta \stackrel{\text{def}}{=} \frac{m}{a}. \quad (8)$$

Note that $\tau_\beta > 0$, since $m > 0$ and $a > 0$. As a consequence, the characteristic equation (3) becomes

$$D(\lambda) = \lambda + 1 - \alpha e^{-\lambda \tau_\alpha} - \beta \frac{a^m}{(\lambda + a)^m} = 0. \quad (9)$$

It is important to note that $D(\lambda)$ is analytic in $\text{Re}(\lambda) > -a$.

The boundary of the stability region will be determined by curves where the characteristic equation has one or more eigenvalues with zero real part. The main goal of this section is to give a concrete description of these curves. To begin, we consider the case of a zero eigenvalue. Setting $\lambda = 0$ in equation (9) shows that this will occur when $\beta = 1 - \alpha$.

The curves where pure imaginary eigenvalues occur are more complicated. In equation (9), we set $\lambda = i\omega$, $\omega > 0$, to obtain

$$i\omega + 1 - \alpha e^{-i\omega \tau_\alpha} - \beta \frac{a^m}{(i\omega + a)^m} = 0. \quad (10)$$

We define

$$\tan \theta \stackrel{\text{def}}{=} \frac{\omega}{a}, \quad (11)$$

and note that $\omega > 0, a > 0$ ($\tau_\beta > 0$) imply that $\theta \in (2k\pi, (2k + \frac{1}{2})\pi)$, $k \in \mathbb{Z}^+ \cup \{0\}$. Substituting this into equation (10), rearranging, and decomposing into real and imaginary components, we arrive at the system:

$$\begin{aligned} 1 - \alpha \cos(\omega \tau_\alpha) - [\omega + \alpha \sin(\omega \tau_\alpha)] \tan(m\theta) - \beta r &= 0, \\ \omega + \alpha \sin(\omega \tau_\alpha) + [1 - \alpha \cos(\omega \tau_\alpha)] \tan(m\theta) &= 0, \end{aligned} \quad (12)$$

where $r \stackrel{\text{def}}{=} \frac{\cos^m \theta}{\cos m\theta}$. The second equation of system (12) yields

$$\begin{aligned} \tan(m\theta) &= -\frac{\omega + \alpha \sin(\omega \tau_\alpha)}{1 - \alpha \cos(\omega \tau_\alpha)} \\ &\stackrel{\text{def}}{=} h(\omega), \end{aligned} \quad (13)$$

which we substitute back into the first equation in (12) to arrive at

$$\beta \cos^m \theta = \frac{[(\omega + \alpha \sin(\omega \tau_\alpha))^2 + (1 - \alpha \cos(\omega \tau_\alpha))^2]}{(1 - \alpha \cos(\omega \tau_\alpha))} \cos(m\theta). \quad (14)$$

The relation in (12) is manipulated to obtain

$$\beta = \pm \sqrt{(1 - \alpha \cos(\omega \tau_\alpha))^2 + (\omega + \alpha \sin(\omega \tau_\alpha))^2} \cos^{-m} \theta, \quad (15)$$

which is then substituted back into equation (14), giving

$$\cos(m\theta) = \pm \frac{(1 - \alpha \cos(\omega \tau_\alpha))}{\sqrt{(1 - \alpha \cos(\omega \tau_\alpha))^2 + (\omega + \alpha \sin(\omega \tau_\alpha))^2}}. \quad (16)$$

From (8) and (11), we have that

$$\tau_\beta = \frac{m}{\omega} \tan \theta. \quad (17)$$

Equation (13) gives the following representation of θ

$$m\theta = \begin{cases} \text{Arctan}[h(\omega)] + 2l\pi & , \text{ if } \cos(m\theta) \geq 0, \\ \text{Arctan}[h(\omega)] + (2l+1)\pi & , \text{ if } \cos(m\theta) < 0. \end{cases} \quad (18)$$

where $l = 0, 1, 2, \dots$. Employing (16) and (18) in (15) and (17) yields expressions for β and τ_β in terms of (ω, l) and the model parameters. Note that we must restrict ω so that $\tau_\beta > 0$. From (15), (18), and (17), it follows that the 2-tuple $(\beta(\omega, l), \tau_\beta(\omega, l))$ may be ‘periodic’; depending on the values of the indices $m > 0$ and $l \in \mathbb{Z}^+ \cup \{0\}$. As an example, for a given $m \in \mathbb{Z}^+$, the parametric curve $(\beta(\omega, l), \tau_\beta(\omega, l))$ replicates at an l for which: (i) $\frac{2l+1}{m} = 2$, if $\cos(m\theta) < 0$; and (ii) $\frac{2l}{m} = 2$, if $\cos(m\theta) > 0$. In Subsections 3.1 and 3.2, we will attempt to characterise the dynamics of the total number of curves in the $(\beta(\omega, l), \tau_\beta(\omega, l))$ parameter space for $m \in \mathbb{Z}^+$ and a restricted set of parameter values.

3.1. How unique curves are generated in the (β, τ_β) parameter space

This section examines how *unique* 2-tuples (β, τ_β) are generated in the parameter space, as the gamma distribution index $m \in \mathbb{Z}^+$ is varied. These curves represent stability boundaries in the parameter space, and so an analysis of how they evolve is essential in understanding stability properties of the trivial solution of (7). Let us begin by recalling the results of Lemma 1 and noting that the denominator of (13) satisfies $1 - \alpha \cos(\omega\tau_\alpha) \geq 0$ if $|\alpha| \leq 1$. It is clear that if $0 < \alpha \leq \min(1, u^*/\tau_\alpha)$ or $\max(-1, -1/\tau_\alpha) \leq \alpha < 0$, then $h(\omega) \in (-\infty, 0]$ and $\lim_{\omega \rightarrow 0} h(\omega) = 0$. This leads to $\frac{1}{m} \text{Arctan}[h(\omega)] \in \left(-\frac{\pi}{2m}, 0\right]$. In the following description, we consider two cases, namely: $\cos(m\theta) > 0$ and $\cos(m\theta) < 0$. Since $|\alpha| < 1$, the sign of $\cos(m\theta)$ is determined by the choice of \pm in (16). As a consequence, when $\cos(m\theta) > 0$, we have that

$$\begin{aligned} \beta^+(\omega, l^+) &= \sqrt{[1 - \alpha \cos(\omega\tau_\alpha)]^2 + [\omega + \alpha \sin(\omega\tau_\alpha)]^2} \cos^{-m} \theta^+(\omega, l^+), \\ \tau_\beta^+(\omega, l^+) &= \frac{m}{\omega} \tan \theta^+(\omega, l^+), \\ \theta^+(\omega, l^+) &= \frac{\text{Arctan}[h(\omega)]}{m} + \frac{2l^+\pi}{m}, \end{aligned} \quad (19)$$

where we have used the fact that $\cos^m(\theta) > 0$. From this, we observe that $\tau_\beta^+(\omega, 0) = \frac{m}{\omega} \tan\left(\frac{1}{m} \text{Arctan}[h(\omega)]\right) < 0$ for all $m \in \mathbb{Z}^+$. This means that we need to restrict our consideration to $l^+ > 0$.

To understand how unique curves are generated in parameter space, for (19), we need to determine when $(\beta^+(\omega, l^+), \tau_\beta^+(\omega, l^+)) \neq (\beta^+(\omega, l^+ + p), \tau_\beta^+(\omega, l^+ + p))$, where $p \in \mathbb{Z}^+$ is to be determined. If we consider m odd, we see that $\cos^m \theta^+(\omega, l^+)$ is 2π -periodic in θ since

$$\cos^m \theta^+(\omega, l^+) = \frac{1}{2^n} [1 + \cos 2\theta^+(\omega, l^+)]^n \cos \theta^+(\omega, l^+),$$

where $n \in \mathbb{Z}^+ \cup \{0\}$. Now, if we set $p = m$, we note that $\theta^+(\omega, l^+ + m) = \theta^+(\omega, l^+) + 2\pi$, which implies that $\cos^m \theta^+(\omega, l^+) = \cos^m \theta^+(\omega, l^+ + m)$ and $\tan \theta^+(\omega, l^+) = \tan \theta^+(\omega, l^+ + m)$. From this, we obtain that $(\beta^+(\omega, l^+), \tau_\beta^+(\omega, l^+)) = (\beta^+(\omega, l^+ + m), \tau_\beta^+(\omega, l^+ + m))$, which means that the parametric curves for l^+ and $l^+ + m$ are identical. We conclude that parametric curves of the form $(\beta^+(\omega, l^+), \tau_\beta^+(\omega, l^+))$ are distinct for $l^+ = 1, 2, \dots, m-1$, with m fixed. The above analysis is easily extended to the case m even. Here we see that $\cos^m \theta^+(\omega, l^+) = \frac{1}{2^k} [1 + \cos 2\theta^+(\omega, l^+)]^k$, which is clearly π -periodic in θ . Furthermore, we note that $\theta^+(\omega, l^+ + \frac{m}{2}) = \theta^+(\omega, l^+) + \pi$, implying that $(\beta^+(\omega, l^+), \tau_\beta^+(\omega, l^+)) = (\beta^+(\omega, l^+ + \frac{m}{2}), \tau_\beta^+(\omega, l^+ + \frac{m}{2}))$.

m	l^+	l^-
1	none	none
2, 3	none	0
4, 5	1	0
6, 7	1	0, 1
8, 9	1, 2	0, 1
\vdots	\vdots	\vdots

Table 1: Values of l which yield curves with $\tau_\beta > 0$ for various values of m

Therefore, for m even, curves of the form $(\beta^+(\omega, l^+), \tau_\beta^+(\omega, l^+))$ are distinct for $l^+ = 1, 2, \dots, \frac{m}{2} - 1$. We now look at the case $\cos(m\theta) < 0$, for which

$$\begin{aligned}
\beta^-(\omega, l^-) &= -\sqrt{[1 - \alpha \cos(\omega\tau_\alpha)]^2 + [\omega + \alpha \sin(\omega\tau_\alpha)]^2} \cos^{-m} \theta^-(\omega, l^-), \\
\tau_\beta^-(\omega, l^-) &= \frac{m}{\omega} \tan \theta^-(\omega, l^-), \\
\theta^-(\omega, l^-) &= \frac{\text{Arctan}[h(\omega)]}{m} + \frac{(2l^-+1)\pi}{m}.
\end{aligned} \tag{20}$$

By an argument analogous to the one above, we arrive at the following results. For m odd, the curves $(\beta^-(\omega, l^-), \tau_\beta^-(\omega, l^-))$ are distinct for $l^- = 1, 2, \dots, m - 1$. Similarly, for m even, we get that the curves $(\beta^-(\omega, l^-), \tau_\beta^-(\omega, l^-))$ are distinct for $l^- = 1, 2, \dots, \frac{m}{2} - 1$. In conclusion, we note that the total number of distinct curves $(\beta^-(\omega, l^-), \tau_\beta^-(\omega, l^-))$ and $(\beta^+(\omega, l^+), \tau_\beta^+(\omega, l^+))$ in parameter space is influenced only by the index m . It is also clear that the total number of such curves in parameter space increases as m is increased.

3.2. Generation of new curves in the (β, τ_β) parameter space

As m increases, new curves are ‘born’ in the (β, τ_β) parameter space, as suggested by the preceding discussion. Thus, as m increases, so does the number of parametric curves. Recalling that τ_β is restricted to be positive and $\cos^m(\theta) > 0$ shows that the curves $(\beta^+(\omega, l^+), \tau_\beta^+(\omega, l^+))$ lie in the first quadrant, while $(\beta^-(\omega, l^-), \tau_\beta^-(\omega, l^-))$ lie in the second quadrant. It remains to determine how or whether l^+, l^- can be chosen so that $\tau_\beta^+, \tau_\beta^- > 0$. That is, such that $\theta^+(\omega, l^+), \theta^-(\omega, l^-) \in (2k\pi, (2k + \frac{1}{2})\pi)$ for some $k \in \mathbb{Z}^+ \cup \{0\}$.

We begin by recalling that $\frac{1}{m} \text{Arctan}[h(\omega)] \in (-\frac{\pi}{2m}, 0)$. From this, it is evident that $\theta^+(\omega, l^+) = \frac{1}{m} \text{Arctan}[h(\omega)] + \frac{2l^+\pi}{m} \in \frac{\pi}{m} (\frac{4l^+-1}{2}, 2l^+)$. Thus, for θ^+ to overlap in the correct interval (so that $\tau_\beta > 0$), we must have integers m, l^+ , and k such that

$$2k\pi \leq \frac{4l^+ - 1}{2m}\pi < (2k + \frac{1}{2})\pi, \quad \text{or} \quad 2k\pi < \frac{2l^+}{m}\pi \leq (2k + \frac{1}{2})\pi.$$

The first of these inequalities is equivalent to

$$mk + \frac{1}{4} \leq l^+ < mk + \frac{1}{4} + \frac{m}{4},$$

from which we conclude that $m \geq 4$ in order for this to be possible. Further, by recalling that $l^+ = 0, \dots, m - 1$, we find that we must have $k = 0$ to satisfy the inequality. A similar analysis of the second inequality yields the same restrictions. Setting $k = 0$, we can determine which values of l^+ generate appropriate values of θ^+ . This is summarised in Table 1.

Similarly, we have that $\theta^-(\omega, l^-) \in \frac{\pi}{m} \left(\frac{4l^+ + 1}{2}, 2l^+ \right)$. Thus, for θ^- to be in the appropriate interval so that $\tau_\beta > 0$, we require that

$$2k\pi \leq \frac{4l^+ + 1}{2m}\pi < (2k + \frac{1}{2})\pi, \quad \text{or} \quad 2k\pi < \frac{4l^+ + 2}{2m}\pi \leq (2k + \frac{1}{2})\pi.$$

Analysis as above shows that these inequalities can only be satisfied for $m \geq 2$ and $k = 0$. This gives rise to the values of l^- shown in Table 1. Unfortunately, the nonlinearity of the function $h(\omega)$ makes it impossible to analytically compute the ω interval giving rise to the curves described by Table 1. However, the curves can be computed numerically. Figure 2 shows an ensemble of some specific curves in the parameter space (β, τ_β) to give credence to our theoretical results. It is important to note that the only relevant quadrants are the first and the second, since $\tau_\beta > 0$.

3.3. Preservation of stability when traversing curves in parameter space

Starting from the characteristic equation (9), we can divide through by a^m , substitute $\tau_\beta = \frac{m}{a}$, and rearrange to obtain

$$\left(\lambda + 1 - \alpha e^{-\lambda\tau_\alpha} \right) \left(\frac{\lambda\tau_\beta}{m} + 1 \right)^m - \beta = 0. \quad (21)$$

Let us consider first the variation of β . Differentiating equation (21) with respect to β , assuming $\lambda = \lambda(\beta)$, and rearranging yields

$$\frac{d\lambda}{d\beta} = \frac{1}{(1 + \alpha\tau_\alpha e^{-\lambda\tau_\alpha}) \left(\frac{\lambda\tau_\beta}{m} + 1 \right) + \tau_\beta (\lambda + 1 - \alpha e^{-\lambda\tau_\alpha})}. \quad (22)$$

Substituting $\lambda = 0$ then leads to

$$\left. \frac{d\lambda}{d\beta} \right|_{\lambda=0} = \frac{1}{1 + \alpha\tau_\alpha + \tau_\beta (1 - \alpha)}. \quad (23)$$

Thus, along the line $\beta = 1 - \alpha$, we have

$$\frac{d\lambda}{d\beta} \begin{cases} > 0 & \text{if } 0 \leq \alpha < 1 \\ \geq 0 & \text{if } \alpha > 1 \text{ and } \tau_\beta \geq \frac{1 + \alpha\tau_\alpha}{\alpha - 1} \\ \geq 0 & \text{if } \alpha < 0 \text{ and } \tau_\beta \leq \frac{1 + \alpha\tau_\alpha}{\alpha - 1} \end{cases} \quad (24)$$

Differentiating (21) with respect to τ_β , assuming $\lambda = \lambda(\tau_\beta)$, and rearranging gives

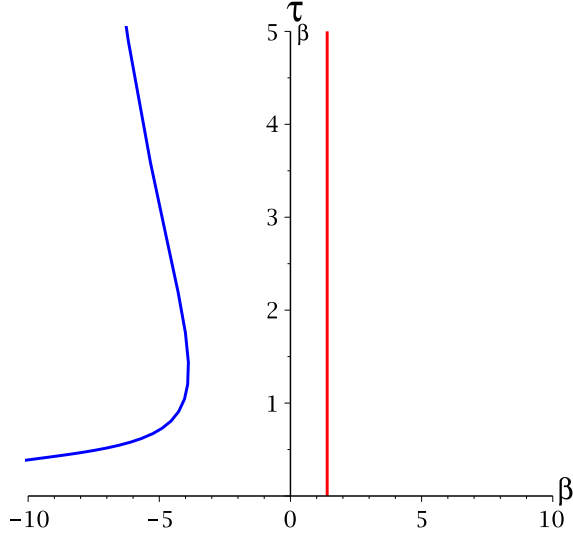
$$\frac{d\lambda}{d\tau_\beta} = \frac{\lambda (\alpha e^{-\lambda\tau_\alpha} - s - 1)}{(1 + \alpha\tau_\alpha e^{-\lambda\tau_\alpha}) \left(\frac{\lambda\tau_\beta}{m} + 1 \right) + \tau_\beta (\lambda + 1 - \alpha e^{-\lambda\tau_\alpha})}. \quad (25)$$

Substituting $\lambda = i\omega$, $\omega > 0$, gives the following.

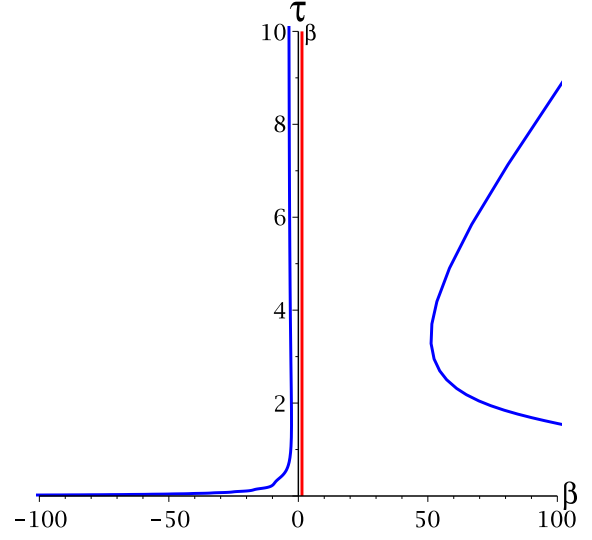
$$\left(\frac{d\lambda}{d\tau_\beta} \right) \Big|_{\lambda=i\omega} = \frac{i\omega (\alpha e^{-i\omega\tau_\alpha} - i\omega - 1)}{(1 + \alpha\tau_\alpha e^{-i\omega\tau_\alpha}) \left(\frac{i\omega\tau_\beta}{m} + 1 \right) + \tau_\beta (i\omega + 1 - \alpha e^{-i\omega\tau_\alpha})}. \quad (26)$$

This leads to

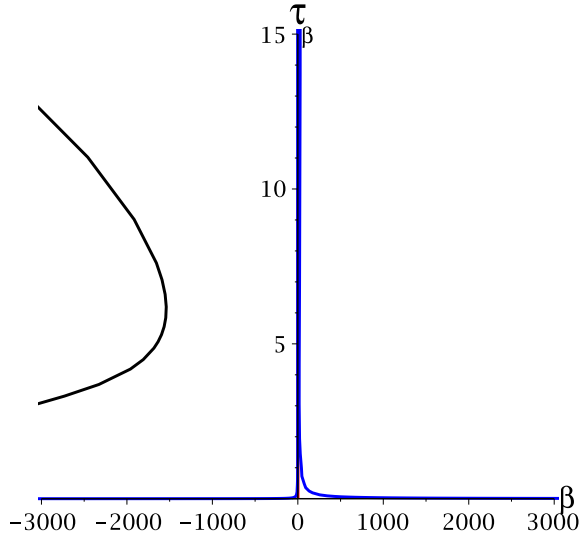
$$\text{Re} \left(\frac{d\lambda}{d\tau_\beta} \Big|_{\lambda=i\omega} \right) = \frac{AC + BD}{C^2 + D^2}, \quad (27)$$



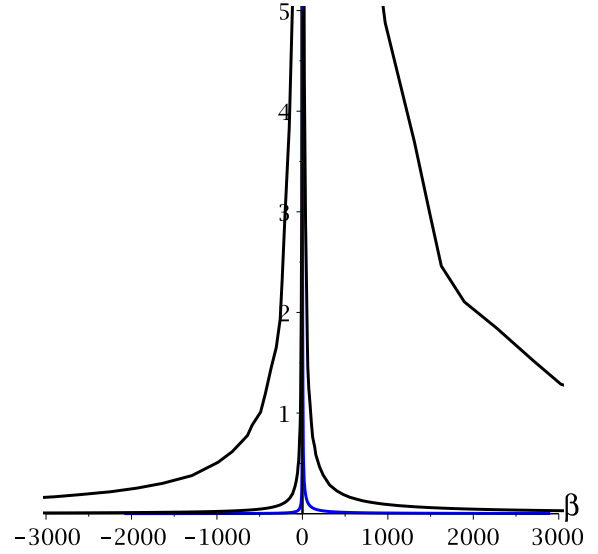
(a) $m = 3$.



(b) $m = 5$.



(c) $m = 7$.



(d) $m = 30$.

Figure 2: A display of some bifurcation curves (blue, black) in the (β, τ_β) parameter space, with m as indicated. The parameters used here are $\alpha = -0.4$, $\tau_\alpha = 1$ and l as shown in Table 1. The range of $\omega > 0$ was varied to accommodate different scales. Only six of 15 curves for $m = 30$ appear at the chosen scale. The red line is the line $\beta = 1 - \alpha$.

where

$$\begin{aligned}
 A &= \omega[\omega + \alpha \sin(\omega\tau_\alpha)] , \\
 B &= \omega[\alpha \cos(\omega\tau_\alpha) - 1] , \\
 C &= 1 + \alpha\tau_\alpha \cos(\omega\tau_\alpha) + \frac{\alpha\omega\tau_\beta\tau_\alpha}{m} \sin(\omega\tau_\alpha) + \tau_\beta [1 - \alpha \cos(\omega\tau_\alpha)] \\
 &= \frac{\alpha}{a}(a\tau_\alpha - m) \cos(\omega\tau_\alpha) + \frac{\alpha\omega\tau_\alpha}{a} \sin(\omega\tau_\alpha) + \frac{1}{a}(m + a) , \\
 D &= -\alpha\tau_\alpha \sin(\omega\tau_\alpha) + \frac{\omega\tau_\beta}{m} [1 + \alpha\tau_\alpha \cos(\omega\tau_\alpha)] + \tau_\beta [\omega + \alpha \sin(\omega\tau_\alpha)] \\
 &= \frac{\alpha}{a}(m - a\tau_\alpha) \sin(\omega\tau_\alpha) + \frac{\alpha\omega\tau_\alpha}{a} \cos(\omega\tau_\alpha) + \frac{\omega}{a}(1 + m) .
 \end{aligned} \tag{28}$$

We note that the numerator of the right hand side of (27) is given by

$$AC + BD = \alpha\omega\tau_\alpha [\sin(\omega\tau_\alpha) + \omega \cos(\omega\tau_\alpha)] + \frac{\alpha\omega^2}{a}(1 - \tau_\alpha) \cos(\omega\tau_\alpha) + \frac{\alpha\omega}{a}(\omega^2\tau_\alpha + a) \sin(\omega\tau_\alpha) + \frac{\omega^2}{a}(a - 1 + \alpha^2\tau_\alpha). \quad (29)$$

We will show how $\operatorname{Re}\left(\frac{d\lambda}{d\tau_\beta}\Big|_{\lambda=i\omega}\right)$ is related to $\frac{d\beta^\pm}{d\omega}$. Differentiation of (15) with respect to ω leads to

$$\frac{d\beta^\pm}{d\omega} = \beta^\pm \left[\frac{\hat{A}\hat{A}' + \hat{B}\hat{B}'}{\hat{A}^2 + \hat{B}^2} + m \tan(\theta) \frac{d\theta}{d\omega} \right], \quad (30)$$

where $\hat{A} := A/\omega$ and $\hat{B} := B/\omega$. Using equations (11) and (13), and simplifying, we arrive at

$$\begin{aligned} \frac{d\beta^\pm}{d\omega} &= \frac{\beta^\pm}{\hat{A}^2 + \hat{B}^2} \left[\omega + \alpha \sin(\omega\tau_\alpha) + \alpha\tau_\alpha [\sin(\omega\tau_\alpha) + \omega \cos(\omega\tau_\alpha)] \right. \\ &\quad \left. + \frac{\omega}{a} (\alpha(1 - \tau_\alpha) \cos(\omega\tau_\alpha) + \alpha\tau_\alpha\omega \sin(\omega\tau_\alpha) + \alpha^2\tau_\alpha - 1) \right] \\ &= \omega\beta^\pm \left(\frac{AC + BD}{A^2 + B^2} \right). \end{aligned} \quad (31)$$

By substituting (31) into (27), we arrive at the expression

$$\operatorname{Re}\left(\frac{d\lambda}{d\tau_\beta}\Big|_{\lambda=i\omega}\right) = \frac{1}{\omega\beta^\pm} \left(\frac{A^2 + B^2}{C^2 + D^2} \right) \frac{d\beta^\pm}{d\omega}. \quad (32)$$

From the relationship (32), $\beta^+ > 0$, $\beta^- < 0$, and $\omega > 0$, it is clear that

$$\operatorname{Re}\left(\frac{d\lambda}{d\tau_\beta}\Big|_{\lambda=i\omega}\right) \gtrless 0 \iff \frac{d\beta^+}{d\omega} \gtrless 0 \text{ or } \frac{d\beta^-}{d\omega} \lesseqgtr 0. \quad (33)$$

This leads to the following proposition.

Proposition 1. *The number of roots of the characteristic equation (9) with positive real parts is increasing/decreasing when $\beta^+(\omega)$ is an increasing/decreasing function of ω and the opposite for $\beta^-(\omega)$.*

4. Exact Stability Region

We are now in a position to more fully describe the region in the (β, τ_β) parameter space where the trivial solution of (7) is asymptotically stable. We will do so by putting together the results of Theorems 2.1-2.2 and Proposition 1 and the description of the curves where the characteristic equation has a pair of pure imaginary roots.

4.1. The case $m = 1$.

When $m = 1$ the analysis simplifies considerably. In this case there can be at most one curve along which the characteristic equation has a pair of pure imaginary roots. We describe this curve and how/when it forms part of the boundary of the stability region below.

To begin, we set $m = 1$ and $\tau_\beta = 1/a$ in equations (11), (13) and (14) to obtain

$$\tau_\beta = \frac{h(\omega)}{\omega} \quad (34)$$

$$\beta = \frac{(1 - \alpha \cos(\omega\tau_\alpha))^2 + (\omega + \alpha \sin(\omega\tau_\alpha))^2}{1 - \alpha \cos(\omega\tau_\alpha)} = (1 - \alpha \cos(\omega\tau_\alpha)) + \frac{(\omega + \alpha \sin(\omega\tau_\alpha))^2}{1 - \alpha \cos(\omega\tau_\alpha)} \quad (35)$$

where $h(\omega)$ is given by (13). For fixed α and τ_α , these equations define a curve in the β, τ_β parametrically in terms of ω . Further, note the following limits.

$$\lim_{\omega \rightarrow 0} \tau_\beta(\omega) = \lim_{\omega \rightarrow 0} \frac{-(1 + \alpha\tau_\alpha \frac{\sin(\omega\tau_\alpha)}{\omega\tau_\alpha})}{1 - \alpha \cos(\omega\tau_\alpha)} = -\frac{1 + \alpha\tau_\alpha}{1 - \alpha}, \quad (36)$$

$$\lim_{\omega \rightarrow 0} \beta = 1 - \alpha,$$

and

$$\tau_\beta = 0 \Rightarrow h(\omega) = 0 \Rightarrow \omega + \alpha \sin(\omega\tau_\alpha) = 0 \Rightarrow \beta = 1 - \alpha \cos(\omega\tau_\alpha)$$

This leads to the following.

Proposition 2. *If $m = 1$, $0 < \alpha < 1$ and $\tau_\alpha \geq 0$, then the trivial solution is asymptotically stable in the region $\beta < 1 - \alpha$, $\tau \geq 0$.*

Proof. In this case, from equation (35) $\beta \geq 1 - \alpha > 0$. Thus the curve (β, τ_β) defined by (34)-(35) can only lie in Quadrants I or IV. Since in Quadrant I the curve lies to the right of the curve $\beta = 1 - \alpha$, by Theorem 2.1 it won't affect the stability and the result follows. ■

Proposition 3. *If $m = 1$, $-1 < \alpha < 0$ and $\tau_\alpha \leq -1/\alpha$, then the trivial solution is asymptotically stable in the region $\beta < 1 - \alpha$, $\tau \geq 0$.*

Proof. In this case, from equation (35) $\beta > 1 + \alpha > 0$. So the curve can only lie in Quadrant I or IV. By Lemma 1 $h(\omega) < 0$ for all $\omega > 0$, which implies that $\tau_\beta < 0$ for all $\omega > 0$, i.e., the curve lies in Quadrant IV. Hence it does not affect the stability. The result then follows from Theorems 2.1 and 2.2. ■

The results of Propositions 2-3 are shown in Figure 3(a).

Proposition 3 requires $|\alpha\tau_\alpha|$ small enough for stability. If $\tau_\alpha > -1/\alpha$ then $\tau_\beta > 0$ as $\omega \rightarrow 0$ and part of the curve lies in Quadrant I starting on the line $\beta = 1 - \alpha$ and ending the right of the line $\beta = 1 + \alpha$. Consideration of the results of the previous section shows that the stability region lies outside this curve. See Figure 3(b).

When $|\alpha| > 1$ the curve has discontinuities when $1 - \alpha \cos(\omega\tau_\alpha) = 0$ and the stability boundary becomes more complex. However, we can say the following.

Proposition 4. *If $m = 1$, $\alpha > 1$ and $\tau_\alpha < u^*/\alpha$, then the trivial solution is unstable above the curve defined by equations (34)–(35) for $0 \leq \omega \leq \omega^*$ where u^* is defined in Lemma 1 and ω^* is the smallest positive zero of $1 - \alpha \cos(\omega\tau_\alpha)$.*

Proof. Let $S(\omega)$ be as defined in the proof of Lemma 1 and $C(\omega) = 1 - \alpha \cos(\omega\tau_\alpha)$. Since $\tau_\alpha < u^*/\alpha$, $S(\omega) > 0$ for $\omega > 0$ thus the curve defined by equations (34)–(35) will either lie in Quadrant IV, in which case it does not affect the stability, or in Quadrant II. The branch of the curve for $\omega \in [0, \omega^*, C(\omega)) < 0$ lies in Quadrant II and emanates from the line $\beta = 1 - \alpha$ when $\omega = 0$. As $\omega \rightarrow \omega^*$, $\tau_\beta \rightarrow \infty$ and $\beta \rightarrow -\infty$. Using the results of the previous section shows that stability is lost along this branch of the curve. It can be shown that all other branches of the curve in Quadrant II lie below this curve. The result follows. ■

(a) $0 \leq \alpha < 1, \tau_\alpha \geq 0$ or $-1 < \alpha < 0, \tau_\alpha \leq -1/\alpha$

(b) $-1 < \alpha < 0, \tau_\alpha > -1/\alpha$

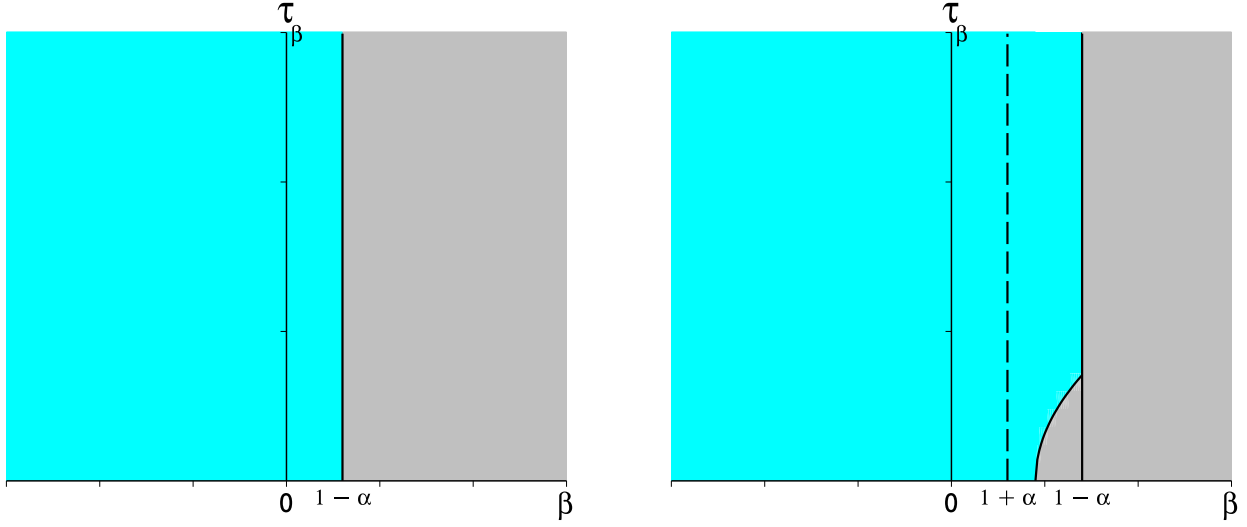


Figure 3: Exact stability regions for $m = 1$ and $|\alpha| < 1$. Regions shaded in grey correspond to instability. Regions shaded in cyan correspond to asymptotic stability

Proposition 5. *If $m = 1$, $\alpha < -1$ and $\tau_\alpha \leq -1/(2\alpha)$, then is the trivial solution is asymptotically stable for $1 + \alpha \leq \beta < 1 - \alpha$.*

Proof. Let $S(\omega)$ be as defined in the proof of Lemma 1 and $C(\omega) = 1 - \alpha \cos(\omega\tau_\alpha)$. Since $\tau_\alpha \leq -1/\alpha$, $S(\omega) > 0$ for $\omega > 0$ thus the curve defined by equations (34)–(35) will either lie in Quadrant IV, in which case it does not affect the stability, or in Quadrant II. Consideration of Theorems 2.1 and 2.3 gives the result. ■

The results of these Propositions are shown in Figure 4. In the white regions of this Figure, the curve defined by (34)–(35) will have an infinite number of branches defined by the ω values where $1 - \alpha \cos(\omega\tau_\alpha) > 0$. Inside these branches trivial solution will be unstable.

4.2. The case $m > 1$.

Our first result shows how Proposition 2 generalises to higher values of m .

Proposition 6. *If $0 < \alpha < 1$ then the right boundary of the region of asymptotic stability of the trivial solution is the line $\beta = 1 - \alpha$. If, in addition, $m = 2, 3, 4, 5$, then the left boundary is the curve $(\beta^-(\omega, 0), \tau_\beta^-(\omega, 0))$.*

Proof. Recall that Theorem 2.1 established that the trivial solution is unstable in the region $\beta > 1 - \alpha$ and that Theorem 2.2 showed that the trivial solution is asymptotically stable for $|\beta| < 1 - |\alpha|$, $\tau_\beta \geq 0$. This stability will be maintained until parameter values where the characteristic equation has a root with zero real part, which occurs along the line $\beta = 1 - \alpha$ or along the curves defined by (19) or (20).

Since $0 < \alpha < 1$, it follows from Theorem 2.2 that the trivial solution is asymptotically stable for $|\beta| < 1 - \alpha$, which gives the first result. Note that this is also confirmed by the fact that, for $0 < \alpha < 1$, the curves (19) satisfy

$$\beta^+(\omega, l^+) \geq (1 - \alpha)$$

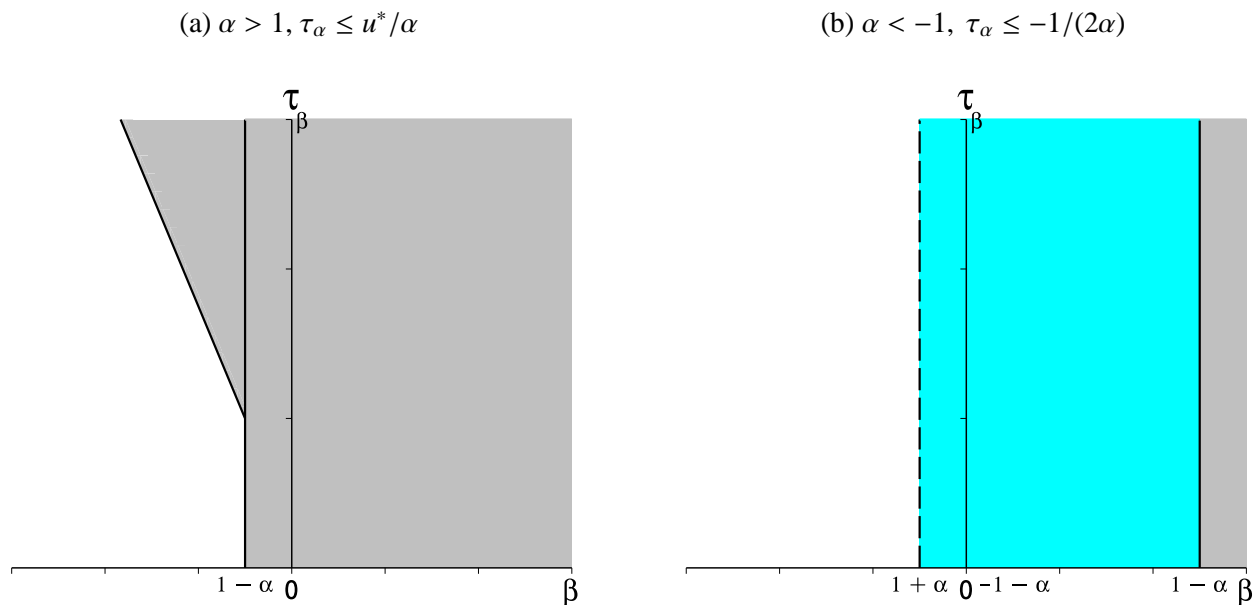


Figure 4: Stability regions for $m = 1$ and $|\alpha| > 1$. Regions shaded in grey correspond to instability. Regions shaded in cyan correspond to asymptotic stability. In the white regions there may be stability or instability depending on the parameter values. See text.

for all l^+ and $m = 1, 2, \dots$. That is, these curves lie to the right of the line $\beta = 1 - \alpha$.

For $m = 2, 3, 4, 5$, from Table 1 there is one curve of (20) lying in the second quadrant, $(\beta^-(\omega, 0), \tau_\beta^-(\omega, 0))$. Thus this curve must form the left boundary of the stability region. ■

The results of Proposition 6 are illustrated in Figure 5. Once one has determined the curves where the characteristic equation has pure imaginary eigenvalues, the stability region can be determined by using Theorems 2.1-2.3 and Proposition 1. It is possible to make general statements about the stability region under conditions other than those of Proposition 6, but such statements become more complicated as the index m increases. Instead, we will make some observations about various cases and illustrate them with examples.

Proposition 6 may be generalised to higher values of m , but the left boundary of the stability region may consist of multiple curves; see Figure 6(a) for an example. It appears that Proposition 6 has an analogue for $-1 < \alpha < 0$ and τ_α sufficiently small. See Figure 2, where in all cases, the stability region is schematically the same as depicted in Figure 5. However, for large enough m or τ_α , this is no longer true; see Figure 6(b) for an example.

Our results for $m > 1$ are all for $|\alpha| \leq 1$. In the case that $|\alpha| > 1$, the expressions for β^\pm and τ_β^\pm are as given in (19)-(20). However, the expressions for θ^\pm are modified to

$$\theta^\pm(\omega, l^\pm) = \begin{cases} \frac{1}{m} \text{Arctan}[h(\omega)] + 2l\pi & , \quad \text{if } \pm(1 - \alpha \cos \tau_\alpha) \geq 0, \\ \frac{1}{m} \text{Arctan}[h(\omega)] + (2l + 1)\pi & , \quad \text{if } \pm(1 - \alpha \cos \tau_\alpha) < 0. \end{cases}$$

Using these expressions we can explore the stability region further. It does appear that Proposition 4 may be generalised to higher values of m , but possibly with a more complicated left boundary of the stability region. This scenario is exemplified in Figure 6(c). One can use the fact [14] that when $\beta = 0$, the trivial solution is asymptotically stable if $\alpha < -1$ and

$$\tau_\alpha < \frac{1}{\sqrt{\alpha^2 - 1}} \arccos\left(\frac{1}{\alpha}\right) = \tau_{crit}.$$

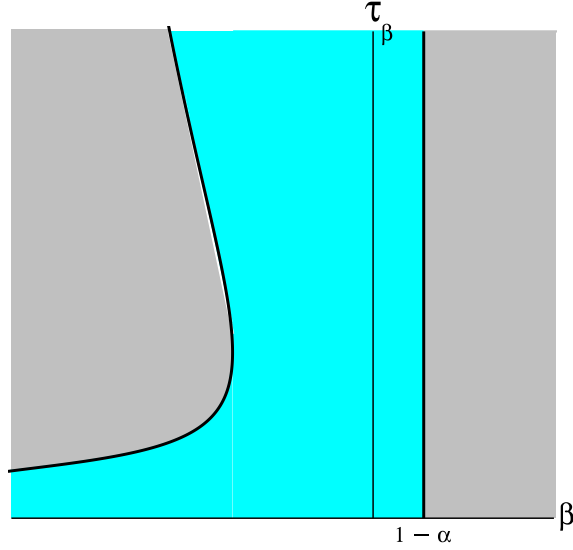


Figure 5: Stability region for $m = 2, 3, 4, 5$ with $0 < \alpha < 1$.

In this situation, the boundary of the stability region will be formed by the parts of the curves of pure imaginary eigenvalues and the line $\beta = 1 - \alpha$ closest to the β axis. An example of this is shown in Figure 6(d), where $-1/\alpha < \tau_\alpha < \tau_{crit}$.

5. Conclusions

We have studied the stability of the trivial solution of a linear, scalar delay differential equation with two distributed time delays. We first gave *distribution-independent* conditions for stability and instability. These conditions are identical to the delay-independent conditions given for a scalar equation with two discrete time delays [12, 13], and so our work generalises this result.

We then considered the case in which one time delay was discrete and the other was gamma distributed. We determined the stability region in the parameter space of the strength of the gamma distributed term and the mean of the gamma distributed time delay and considered how this region evolves as the parameters of the discrete time delay term are varied. Our results show that as the parameter m in the gamma distribution gets larger, the stability region shrinks and the boundary of the stability region becomes more complicated. More detail is given below. Our work generalises that of [25] which only considered the case $m = 1$.

It is important to note that the parameter m in the gamma distribution is a measure of the variance of the distribution, with smaller m yielding a distribution more tightly clustered around the mean. In fact, if the mean of the distribution, τ_α , is held fixed, then in the limit as $m \rightarrow \infty$ the gamma distribution approaches a Dirac distribution. In other words, the time delay becomes discrete [29]; see Figure 7(a). It has been shown for systems with a single gamma distributed time delay that some results for the distributed time delay approach those of the discrete time delay in the limit as $m \rightarrow \infty$ [33, 29, 21, 20]. We observe the same phenomenon in our model with one discrete time delay and one gamma distributed time delay. Consideration of the following limits

$$\lim_{m \rightarrow \infty} m \tan\left(\frac{u}{m}\right) = u, \quad \lim_{m \rightarrow \infty} \sec\left(\frac{u}{m}\right)^m = 1$$

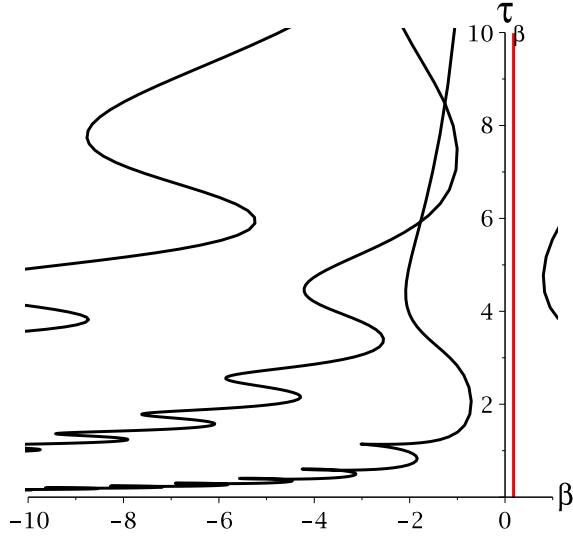
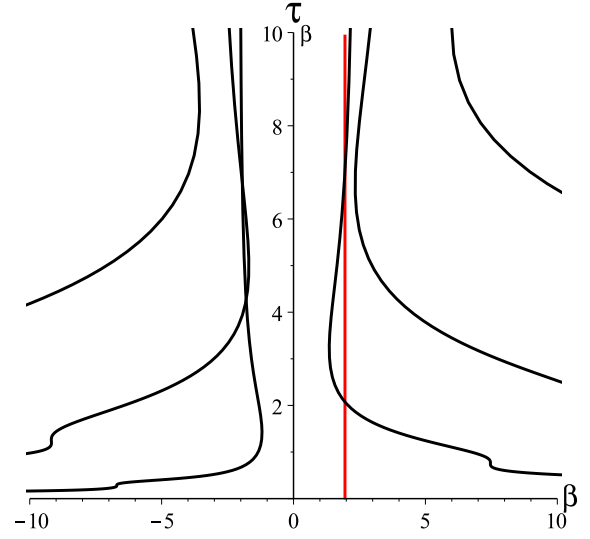
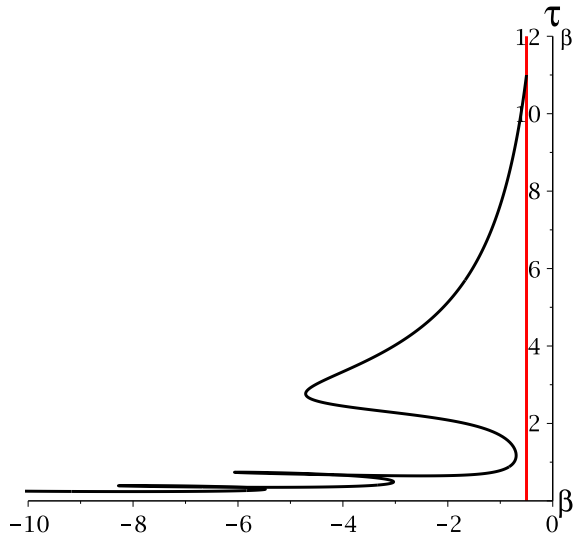
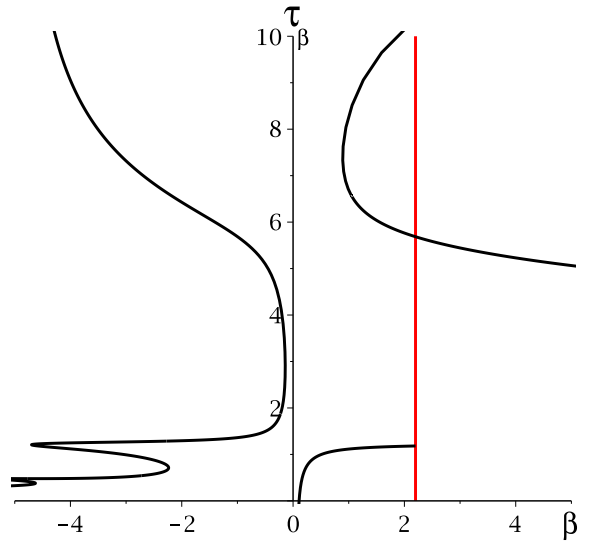
(a) $m = 100, \alpha = 0.95, \tau_\alpha = 4.6$ (b) $m = 100, \alpha = -0.95, \tau_\alpha = 1$ (c) $m = 7, \alpha = 1.5, \tau_\alpha = 3$ (d) $m = 7, \alpha = -1.2, \tau_\alpha = 3$ 

Figure 6: Region of stability of the trivial solution for other parameter values. The boundary of the stability region is made up of the parts of the black curves and the red line which are closest to the τ_β axis. In (a) and (b) different curves correspond to different values of l in the curve equations.

shows that as $m \rightarrow \infty$, the equations for the curves where the characteristic equation (9) has a pair of pure imaginary roots reduce to those for the case of two discrete time delays. These expressions are given by [14]:

$$\beta^\pm(\omega) = \pm \sqrt{[1 - \alpha \cos(\omega\tau_\alpha)]^2 + [\omega + \alpha \sin(\omega\tau_\alpha)]^2},$$

$$\tau_\beta^\pm(\omega, l) = \begin{cases} \frac{1}{\omega} (\text{Arctan}[h(\omega)] + 2l\pi) & , \text{ if } \pm (1 - \alpha \cos(\omega\tau_\alpha)) \geq 0, \\ \frac{1}{\omega} (\text{Arctan}[h(\omega)] + (2l+1)\pi) & , \text{ if } \pm (1 - \alpha \cos(\omega\tau_\alpha)) < 0. \end{cases}$$

As can be seen in Figure 7 (b), the stability region with one distributed time delay and one discrete delay approaches that of a model with two discrete time delays in the limit as $m \rightarrow \infty$.

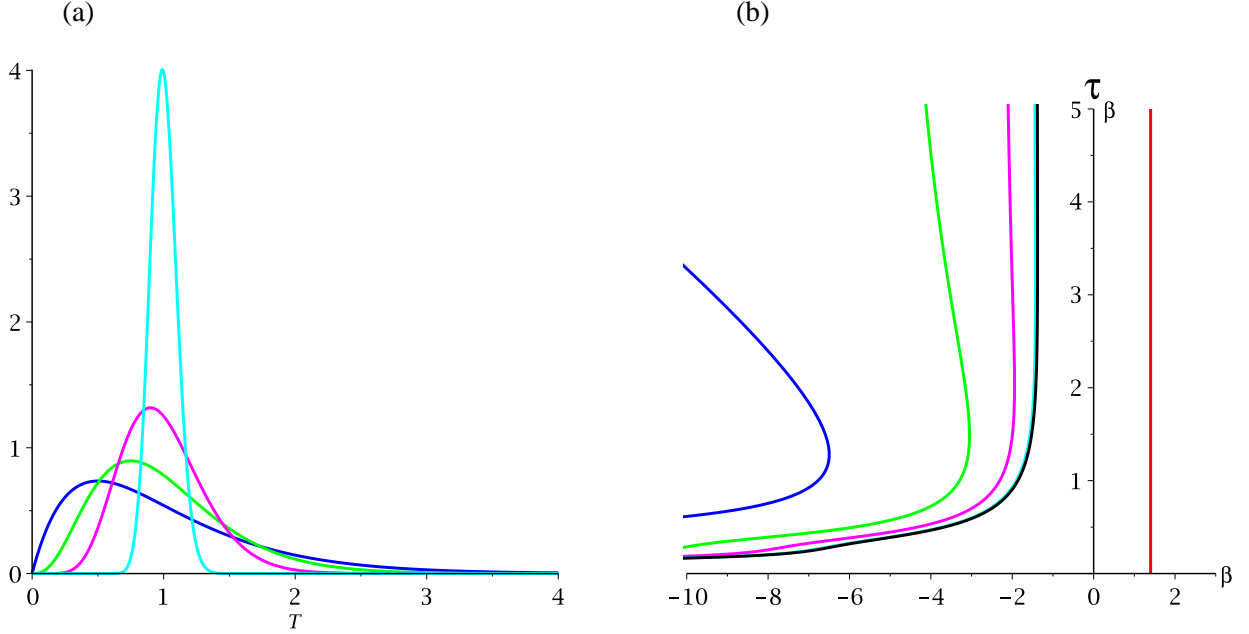


Figure 7: (a) Gamma distributions with $\tau_\alpha = 1$ and $m = 2, 4, 10, 100$. (b) Comparison of the stability region for the model with one discrete and one gamma distributed delay $m = 2, 4, 10, 100$ (blue, green, magenta, cyan) and the model with two discrete delays (black). The other parameters are $\alpha = -0.4, \tau_\alpha = 1$. The red line is the curve $\beta = 1 - \alpha$.

We also observe the following phenomena associated with a differential equation with two discrete time delays [11, 12, 14]. For appropriate parameter values, there is *stability switching*: the trivial solution is asymptotically stable for τ_β small, but then destabilises and re-stabilises a finite number of times as τ_β increases. This can be seen in Figures 6 and 7(b). For τ_α large enough, as depicted in Figure 6, there can be intersection points between different curves forming the boundary of the stability region. These points correspond to parameter values where the characteristic equation has either two pairs of pure imaginary roots (crossing of two black curves) or a pair of pure imaginary roots and a zero root (crossing of black curve and red line). If our characteristic equation were from the linearisation of a nonlinear delay differential equation about an equilibrium point, such points would correspond to points of *codimension two bifurcation* [11].

There are some differences, of course. In the discrete case, if τ_α is small enough stability switching does not occur. This can be seen in Figure 7 (b). The curve which forms the left boundary of the stability region is monotone increasing (thinking of τ_β as a function of β) in the case of a discrete delay, while the curves for the distributed delay are not monotone. Further, when stability switching occurs in the discrete case, it ultimately ends with the trivial solution being unstable [11]. For the distributed case, our observation is that the stability switching sometimes ends with the trivial solution being unstable (see Figures 5 and 7(b)). This is consistent with results of [33] for a system with one time delay. In general, we observe that the stability region for the system with one discrete and one distributed time delay is *larger* than that for two discrete time delays if other parameters are kept fixed. This can be seen in Figure 7(b) and is consistent with the “rule of thumb” that a system with a distributed time delay is inherently more stable than the corresponding system with a discrete time delay. This is shown in many papers including [9, 10, 33, 32, 8] and references therein.

Acknowledgements

All plots were generated using the symbolic algebra package Maple. This work has benefitted from the support of the Natural Sciences and Engineering Research Council of Canada.

References

References

- [1] J. Cushing, *Integrodifferential Equations and Delay Models in Population Dynamics*, Vol. 20 of *Lecture Notes in Biomathematics*, Springer-Verlag, Berlin; New York, 1977.
- [2] T. Faria, J. Oliveira, Local and global stability for lotka-volterra systems with distributed delays and instantaneous negative feedbacks, *J. Diff. Eqs.* 244 (5) (2008) 1049–1079.
- [3] M. Kloosterman, S. Campbell, F. Poulin, A closed NPZ model with delayed nutrient recycling, *J. Math. Biol.* 68 (4) (2014) 815–850.
- [4] Y. Kuang, *Delay Differential Equations with Applications in Population Dynamics*, Academic Press, Boston, 1993.
- [5] S. Bernard, J. Bélair, M. Mackey, Sufficient conditions for stability of linear differential equations with distributed delay, *Discr. Cont. Dyn. Sys.* 1B (2001) 233–256.
- [6] Y. Yuan, J. Bélair, Stability and Hopf bifurcation analysis for functional differential equation with distributed delay, *SIAM J. Appl. Dyn. Sys.* 10 (2) (2011) 551–581.
- [7] R. Jessop, S. Campbell, Approximating the stability region of a neural network with a general distribution of delays, *Neural Networks* 23 (10) (2010) 1187–1201.
- [8] A. Thiel, H. Schwegler, C. Eurich, Complex dynamics is abolished in delayed recurrent systems with distributed feedback times, *Complexity* 8 (4) (2003) 102–108.
- [9] F. Atay, Distributed delays facilitate amplitude death of coupled oscillators, *Phys. Rev. Lett.* 91 (9) (2003) 094101.
- [10] F. Atay, Total and partial amplitude death in networks of diffusively coupled oscillators, *Physica D* 183 (2003) 1–18.
- [11] J. Bélair, S. A. Campbell, Stability and bifurcations of equilibria in a multiple-delayed differential equation, *SIAM J. Appl. Math.* 54 (5) (1994) 1402–1424.
- [12] J. Hale, W. Huang, Global geometry of the stable regions for two delay differential equations, *J. Math. Anal. Appl.* 178 (1993) 344–362.
- [13] J. Mahaffy, P. Zak, K. Joiner, A geometric analysis of stability regions for a linear differential equation with two delays, *Int. J. Bifurc. Chaos* 5 (1995) 779–796.
- [14] Y. Yuan, S. Campbell, Stability and synchronization of a ring of identical cells with delayed coupling, *J. Dyn. Diff. Eqs.* 16 (3) (2003) 709–744.
- [15] O. Diekmann, M. Gyllenberg, Equations with infinite delay: blending the abstract and the concrete, *J. Diff. Eqs.* 252 (2) (2012) 819–851.

- [16] Y. Hino, S. Murakami, T. Naito, Functional differential equations with infinite delay, Springer-Verlag, Berlin, 1991.
- [17] V. Kolmanovskii, A. Myshkis, Introduction to the Theory and Applications of Functional Differential Equations, Vol. 463 of Mathematics and Its Applications, Kluwer, 1999.
- [18] J. Arino, P. van den Driessche, Time Delays in Epidemic Models: Modeling and Numerical Considerations, Springer, Dordrecht, 2006, Ch. 13, pp. 539–558.
- [19] S. Ruan, Delay Differential Equations for Single Species Dynamics, Springer, Dordrecht, 2006, Ch. 11, pp. 477–515.
- [20] G. Wolkowicz, H. Xia, S. Ruan, Competition in the chemostat: A distributed delay model and its global asymptotic behaviour, *SIAM J. Appl. Math.* 57 (1997) 1281–1310.
- [21] G. Wolkowicz, H. Xia, J. Wu, Global dynamics of a chemostat competition model with distributed delay, *J. Math. Biol.* 38 (1999) 285–316.
- [22] R. F. Anderson, Geometric and probabilistic stability criteria for delay systems, *Math. Biosci.* 105 (1) (1991) 81–96.
- [23] R. F. Anderson, Intrinsic parameters and stability of differential-delay equations, *J. Math. Anal. Appl.* 163 (1) (1992) 184–199.
- [24] R. F. Anderson, The relative variance criterion for stability of delay systems, *J. Dyn. Diff. Eqs.* 5 (1) (1993) 105–128.
- [25] I. Ncube, Asymptotic stability in a multiple-delayed scalar differential equation, *Far East J. Dyn. Sys.* 21 (2) (2013) 115–127.
- [26] I. Ncube, Stability switching and Hopf bifurcation in a multiple-delayed neural network with distributed delay, *J. Math. Anal. Appl.* 407 (1) (2013) 141–146.
- [27] K.-W. W. X. Liao, Z. Wu, Bifurcation analysis on a two-neuron system with distributed delays, *Physica D* 149 (2001) 123–141.
- [28] S. Ruan, R. Filfil, Dynamics of a two-neuron system with discrete and distributed delays, *Physica D* 191 (2004) 323–342.
- [29] N. MacDonald, Biological Delay Systems: Linear Stability Theory, Cambridge University Press, Cambridge, 1989.
- [30] N. MacDonald, Time Lags in Biological Models, Vol. 27 of Lecture notes in biomathematics, Springer-Verlag, Berlin; New York, 1978.
- [31] R. Churchill, J. Brown, Complex Variables and Applications, McGraw-Hill, New York, 1984.
- [32] S. Campbell, R. Jessop, Approximating the stability region for a differential equation with a distributed delay, *Math. Meth. Nat. Phenom.* 4 (2) (2009) 1–27.
- [33] K. Cooke, Z. Grossman, Discrete delay, distributed delay and stability switches, *J. Math. Anal. Appl.* 86 (1982) 592–627.